ON THE DESIGN OF AN IMAGE COMPRESSION SCHEME BASED UPON A PRIORI KNOWLEDGE ABOUT IMAGING SYSTEM AND IMAGE STATISTICS

C.H. Slump, F.J. de Bruijn, P.J.A. Hagendoorn
University of Twente, Dept. of Electrical Engineering
Lab. for Network Theory, P.O. Box 217
7500 AE Enschede, the Netherlands
tel.:+31 53-4892094 fax.:+31 53-4891060
e-mail: c.h.slump@el.utwente.nl

ABSTRACT

This contribution is about the design of an image compression scheme for near loss-less image compression of a restricted class of images and a specific application. The images are digital diagnostic X-ray images of the coronary vessels of the human heart. This paper proposes a novel compression scheme with a compression ratio of 8 - 10 with preservation of the diagnostic image quality. Central in our approach is the amount of information a trained and highly skilled observer *i.e.* the cardiologist is able discern at a given exposure and thus quantum noise level. The physics of the image detection process together with the a priori knowledge of the imaging system are the basis of the image statistics. Relevant elements of the human visual system complete the stochastic characterization of imaging process whereon the compression scheme is based.

1. INTRODUCTION

The huge amount of data digitally acquired in diagnostic radiology causes storage problems and in applications such as teleradiology also transmission problems. In some countries the law requires that medical examinations are archived for a period of 20 years. In cardiology images are acquired at 512 times 512 pixels or 1024 times 1024 pixels at 10 bits at a rate of 25 (30) per second. A typical full examination may consist of several runs of more than one minute video in total.

In radiology there is clearly a need for image compression, see [1-4].. However, the images differ very much from the video images existing standards such as JPEG and MPEG are designed for. Especially the noise due to the limited number of X-ray photons has a completely different character and the compression leads to artifacts in the image. Loss less compression schemes give a low compression ratio of about 3 - 4 which is too low. The mentioned standard compression schemes, however, give rise to artifacts which may be diagnostically relevant. Many radiologists and cardiologists oppose lossy image compression. Apart from possible psychological reasons this is due to diagnostic and legal reasons. In the past 20 years the diagnostic imaging equipment has increased in image quality. Also the conversion from film based diagnosis to digital imaging has been accompanied by an increase of the performance. Image compression may be seen as a decrease in performance. This paper will argue that this is not necessarily the case.

The coronary arteries, see Fig. 1, are visualized by angiography, *i.e.* the injection of iodine X-ray contrast material by means of a positioned catheter. The images are

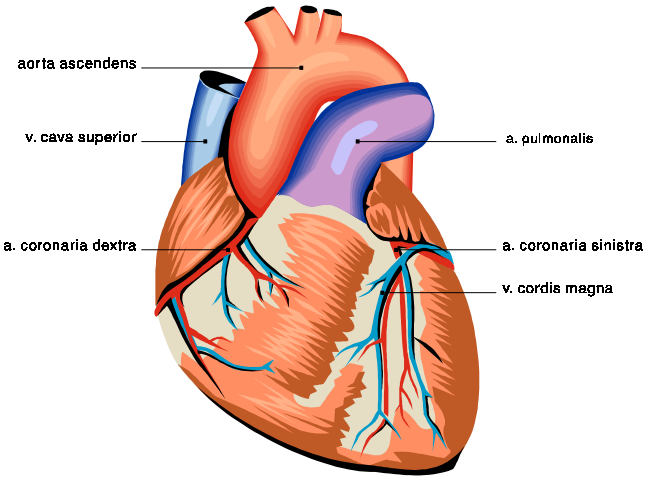

Fig. 1 Overview of the human heart

detected by an image intensifier-television system. The video signals are A to D converted and stored on a disc. The pertinent images do contain a relative large amount of quantum noise due to reasons of dose limitations. The stochastic imaging process is known, the exposures are regulated by means of a known control loop, furthermore, the Modulation Transfer Function (MTF) and the (nonlinear) contrast characteristic function are also known. Based upon this a priori knowledge, a compression scheme is designed for visual loss-less compression. The paper concludes showing results with a typical compression of 10-16, without (too) much visual impairment.

2. IMAGE FORMATION

The images we focus our compression research on are acquired with a Philips Digital Cardiac Imaging (DCI) system. The block diagram of the system is shown in Fig.2. X-ray pulses are generated (typical 5-8 ms) at a rate of 15 - 30 frames per second with the purpose to freeze the motion of the coronary vessels. These arteries are injected with an iodine containing X - ray contrast agent by means of an inserted catheter.

The X- ray photons that have traversed the patient are detected by the image intensifier and converted into a video image by the mounted TV camera. The resulting video signal is digitized in 8 bits after analog preprocessing. The images are stored on a real time digital disk in 512 by 512 format in 8 bit per pixel up to 50 (60) frames per second. The images are processed before they are shown on the monitor such that the low pass Modulation Transfer Function of the system is compensated.

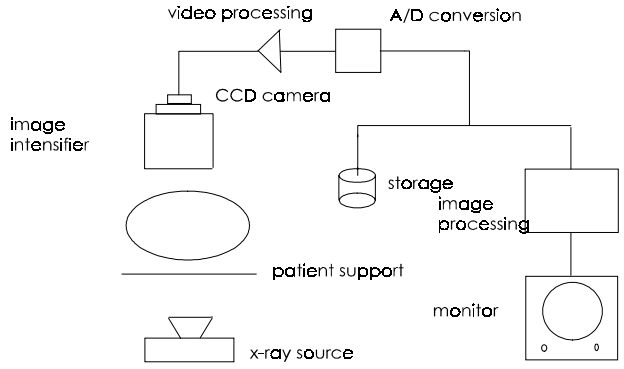

Fig. 2 Block diagram of the diagnostic image acquisition system.

Angiography is imaging of blood vessels filled with contrast material. A simple one dimensional model [5] is illustrated in Fig. 3. We have a cylinder with a certain concentration of iodine representing the blood vessel embedded in a slab of absorbing material simulating the human body. We assume here a parallel monoenergetic exposing X - ray beam and neglect scatter. We model the surrounding tissue by water. The exposing X-ray beam is characterized by the photon fluence Φ_0. The transmitted X-ray photon fluence distribution $\Phi(x)$ equals:

$$\Phi(x) = \Phi_b \; e^{-\alpha\, p(x)}, \qquad (1)$$

with Φ_b denoting the attenuated photon fluence behind the slab in the background and with α the attenuation coefficient of the iodine concentration and with p(x) the traversed distance through the vessel with radius *r* given by:

$$p(x) = 2r \sin(\arccos(\frac{x}{r})) \qquad (2)$$

For $|x| > r$, $p(x) = 0$.

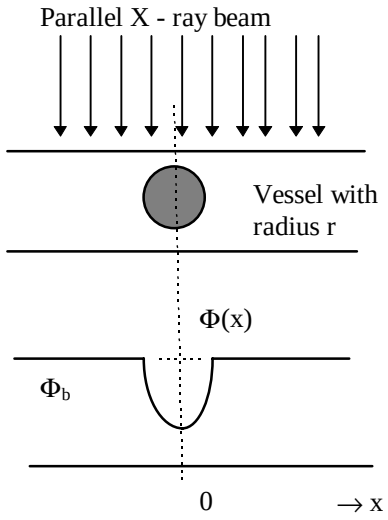

Fig. 3 Cylinder model of angiography.

The transmitted X-ray fluence pattern constitutes the input contrast C to the image intensifier - CCD camera system:

$$C(x) = \frac{\Phi_b - \Phi(x)}{\Phi_b} = 1 - e^{-\alpha\, p(x)} \approx \alpha\; p(x) \qquad (3)$$

for small values of the product α p(x).

The number of X-ray photons n_l impinging per pixel is Poisson distributed:

$$P\{n_l = k\} = e^{-\lambda_l} \; \frac{\lambda_l^k}{k!} \qquad k = 0, 1, 2, \cdots \qquad (4)$$

with λ_l the average number of photons per pixel:

$$\lambda_l = \int_{x_l - 0.5\Delta_{pixel}}^{0.5\Delta_{pixel}} \Phi(x)\, dx \qquad (5)$$

At typical exposure levels in Europe we have for an effective photon energy of 75 keV and a photon fluence Φ of approximately 3×10^4 / m^2 / μR about 100 photons impinging per pixel of a 150 mm diameter input field imaged with a 512×512 CCD sensor matrix.

With an ideal image detector we obtain for a coronary artery with a diameter of 1 mm filled with an iodine concentration of 370 mg I / ml and an effective iodine mass attenuation coefficient of 10 cm^2 / g the maximum contrast value of 69%.

With an average number of photons per pixel of 100, a contrast step of 31% which is about 3 times the standard deviation $\sqrt{100} = 10$ should be visible.

This is in agreement with the Rose model [6] for contrast perception which applied to radiology as a rule of thumb states that for a contrast of 1% and an object diameter of interest to be detected of 1 mm and a noise level (k factor)

of 0.2 times the contrast step, the detected fluence has to be approximately 1 mR. In practice there are also X-ray photons that scatter and this reduces the contrast substantially.
Non ideal imaging system do blur the detected image. Here we are dealing with the low pass behavior of the system only and neglect the additional blurring effect due to the finite size of the focal spot.
With h(x) the point spread function of the image detection system consisting of the image intensifier and the CCD camera we obtain following Papoulis [7] for the expectation value of the detected image I_l with η the Detective Quantum Efficiency (DQE) and c a scaling constant:

$$E\{I_l\} = \eta c \int_{x_l - 0.5\Delta_{pixel}}^{0.5\Delta_{pixel}} dx \int_{-\infty}^{\infty} h(x' - x)\, \Phi(x')\, dx' \quad (6)$$

The detected quantum fluence is convolved with the blurring point spread function. The spatial frequency response of the imaging system is usually characterized by the so called Modulation Transfer Function (MTF) which is the modulus of the Fourier transform of the point spread function. The MTF of the system our images are acquired with is given by [8]:

$$MTF(\nu) = e^{-(\frac{\nu}{\nu_c})^2} \quad (7)$$

with ν the spatial frequency and ν_c a system parameter, in our case [9] equal to 0.94.
Equation (7) clearly shows the low pass behavior of the imaging system which reduces the contrast resolution even more than predicted by the Rose model [6] only.

3. IMAGE COMPRESSION

The previous section explains that with the object modulated X-ray exposure of (on average) 16 μR / frame we obtain coronary angiograms in which shot noise is clearly manifest. The statistical fluctuation in the background is about 10%.
It is well known [6] that human observers are able to detect contrasts if the contrast is several times larger than the statistical fluctuation of the background. For circular structures like nodules, literature reports a factor of 3 - 5. Our images consist of connected tubes, the necessary k factor will be somewhat lower in the order of 2 - 3 .
Computer assisted detection becomes possible if the product of contrast C and the object size d (mm) is greater or equal to unity [10].
Both the shot noise and the low pass imaging do cause standard image compression schemes less suitable. Compression strategies based upon transform coding usually omit higher spatial frequency components and thus cause more blurring of edges. Also filtered noise can give rise to annoying artifact structures.
The common practice of digital diagnostic imaging is that the images are “unsharp masked” before viewing. In this procedure [11] the higher spatial frequencies are enhanced, in partial compensation of low pass imaging system. Noise artifacts and blocking structures from transform coding are also enhanced in this way and become more conspicuous too.
The novel compression scheme is based upon the contrast resolution of the imaging system and contains the following elements:

- The imaging X-ray photons have interacted with the anatomical structure of the patient and are therefore the information carriers. The applied dose determines the quantum noise and together with the MTF (viz. eq. 7) the detectable contrast resolution.
- The acquired image is a realization of a stochastic Poisson process, the first order characteristic of this process is given by eq. 6
- In addition to the quantum noise the images also contain contribution from electrical noise mainly pre amplifier noise and some dark current from the CCD camera.
- Vessels with a diameter < 1 mm are in cardiology not of interest because stenoses in these vessels are hardly detectable and are beyond treatment by e.g. balloon angioplasty (PTCA).
- The compression scheme reduces the contrast resolution of the small clinically not relevant vessel parts. This makes the images less noisy and more suitable for image compaction algorithms.

The outline of the compression algorithm is:

- Convolution of the image with a kernel related to the minimal size of the diagnostic relevant structure, for example vessels with a diameter < 1 mm.
- Comparison on a pixel by pixel basis with threshold levels set by the predicted contrast resolution, viz. Fig. 3 and eq. 6, [12,13].
- Pixel values above the computed threshold level representing the large stuctures with small contrasts or the smaller structures with higher contrast values are left unchanged, the others are replaced by the local average or median values surrounding the pertinent pixel.

The resulting image contains less noise, however, the edges of the clinically relevant vessels are not affected. This is a better entry point for image compression. In the experiment shown in the next section we use a standard DCT compaction algorithm. For more details about this transform coding algorithm we refer to the pertinent literature.In the next section we apply this method to a coronary angiogram, see fig. 4.

4. RESULTS

a

b

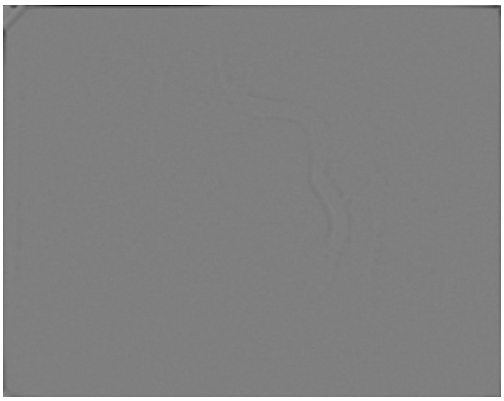

c

Fig4. Typical example of a right coronary angiogram, original (a), reconstruction (b), (mid gray) plus the difference between original and reconstruction (c).

In fig. 4a a typical example of a right coronary angiogram is displayed. Fig 4b shown the reconstructed result after compression with a factor of 16. There ia hardly any impairment of the image visible nor is there any artifact structure manifest. Fig. 4c shows the difference between reconstruction and original angiogram. The difference is mainly noise and there is hardly any anatomical structure visible in this difference image.

REFERENCES

1. S. Wong, L. Zaremba, D. Gooden, H.K. Huang, Radiological image compression - a review, Proc. IEEE, vol. 83, pp. 194-219, 1995
2. M. Breeuwer, R. Heusdens, P. Zwart, Overlapped transform coding of medical x-ray images. In: Yongmin Kim, ed. SPIE Medical Imaging 1994, vol. 2194, pp. 264-275, 1994.
3. M. Das, S. Burgett, Lossless compression of medical images using 2D multiplicative autoregresive models. IEEE Med. Imag., 12, pp. 721-726, 1994.
4. Advances in image and video compression, Proc. IEEE, special issue, Eds. Y.-Q. Zhang, W. Li, M.L. Liou, vol. 83, Feb. 1995.
5. C.E. Metz, K. Doi, Transfer function analysis of radiographic imaging systems, Phys. Med. Biol., vol. 24, pp.1079-1106, 1979.
6. A. Rose, Vision, human and electronic, Plenum Press, New York, 1973.
7. A. Papoulis, Probability, Random Variables and Stochastic Processes, McGraw Hill, New York, 1965.
8. L.A.J. Verhoeven, Digital Subtraction Angiography, Thesis, Technical University Delft, The Netherlands, 1985.
9. M. Brok, C.H. Slump, Automatic determination of image quality parameters in digital radiographic imaging systems, SPIE vol. 1090 Medical Imaging III: Image Formation, pp. 246-256, 1989.
10. C.H. Slump, H.A. Ferwerda, Statistical aspects of image handling in low dose electron microscopy of biological material, Adv. Electronics and Electron Physics, vol. 66, pp.201-308, 1986.
11. W.K. Pratt, Digital image processing, Wiley, New York, 1978
12. H.A. Ferwerda, C.H. Slump, Application of hypothesis testing to electron microscopy, in: Image and signal processing in electron microscopy, p. 113, ed. P.W. Hawkes et al., Scanning Microscopy , Chicago, 1988
13. G.O. Glentis, C.H. Slump, O.E. Herrmann, A versatile algorithm for 2D symmetric noncausal modeling, In: 1994 IEEE Int. Conf. On Image Processing, vol. II, pp 595-599, 1994